Original Article

J Korean Soc Radiol 2024;85(1):184-196
https://doi.org/10.3348/jksr.2023.0065
eISSN 2951-0805

JOURNAL of THE KOREAN SOCIETY of RADIOLOGY

Diagnostic Performance Using a Combination of MRI Findings for Evaluating Cognitive Decline

인지기능 저하평가를 위한 MR 영상 소견 조합의 진단능

Jin Young Byun, MD, Min Kyoung Lee, MD*, So Lyung Jung, MD

Department of Radiology, The Catholic University of Korea, College of Medicine, Yeouido St. Mary's Hospital, Seoul, Korea

ORCID iDs
Jin Young Byun https://orcid.org/0009-0000-5532-2734
Min Kyoung Lee https://orcid.org/0000-0003-3172-3159
So Lyung Jung https://orcid.org/0000-0002-3267-8399

Received June 1, 2023
Revised June 26, 2023
Accepted July 8, 2023

***Corresponding author**
Min Kyoung Lee, MD
Department of Radiology,
The Catholic University of Korea,
College of Medicine,
Yeouido St. Mary's Hospital,
10 63-ro, Yeongdeungpo-gu,
Seoul 07345, Korea.

Tel 82-2-3779-2411
Fax 82-2-783-5288
E-mail tosky333mk@gmail.com

Purpose We investigated potentially promising imaging findings and their combinations in the evaluation of cognitive decline.

Materials and Methods This retrospective study included 138 patients with subjective cognitive impairments, who underwent brain MRI. We classified the same group of patients into Alzheimer's disease (AD) and non-AD groups, based on the neuropsychiatric evaluation. We analyzed imaging findings, including white matter hyperintensity (WMH) and cerebral microbleeds (CMBs), using the Kruskal–Wallis test for group comparison, and receiver operating characteristic (ROC) curve analysis for assessing the diagnostic performance of imaging findings.

Results CMBs in the lobar or deep locations demonstrated higher prevalence in the patients with AD compared to those in the non-AD group. The presence of lobar CMBs combined with periventricular WMH (area under the ROC curve [AUC] = 0.702 [95% confidence interval: 0.599–0.806], $p < 0.001$) showed the highest performance in differentiation of AD from non-AD group.

Conclusion Combinations of imaging findings can serve as useful additive diagnostic tools in the assessment of cognitive decline.

Index terms Alzheimer Disease; Cognitive Decline; Magnetic Resonance Image; Cerebral Small Vessel Disease

INTRODUCTION

With the increasing population of older individuals in both developed and developing countries, concerns regarding memory impairment and cognitive decline in these individuals are also growing (1). Multiple ongoing studies are attempting to identify the underlying

causes and effective treatments for various forms of cognitive decline, including Alzheimer's disease (AD) (2-5). Cognitive function tests are usually used for diagnosing cognitive decline (6, 7). Recent studies have demonstrated the additive value of imaging techniques, including functional imaging, PET, and volumetric analysis, for evaluating cognitive declined (8-11). Although advanced imaging technique demonstrated better diagnostic performance compared to conventional imaging, imaging findings via conventional imaging has additive value in evaluating cognitive decline. Moreover, because most institution caring for patients with cognitive declined have certain limitations to performing advanced imaging techniques, visualized estimation using conventional imaging can help evaluate change during follow-up and provide the rationale for tertiary hospital referral.

In previous studies, many authors have already proven that small-vessel disease is an important predisposing factor for cognitive decline (12-15). In this regard, imaging findings, including white matter hyperintensity (WMH) and cerebral microbleeds (CMBs), have been suggested to be imaging findings for small-vessel disease within the brain (16, 17). These imaging findings could be simple visualizing findings for estimating cognitive decline. Although these imaging findings have been individually shown to be correlated with cognitive decline in previous studies (18, 19), no previous studies have evaluated the usefulness of combinations of these imaging findings for the diagnosis of cognitive decline.

Thus, the purpose of this study was aimed to evaluate the diagnostic performance of conventional imaging findings using combination of those findings for estimating cognitive decline.

MATERIALS AND METHODS

STUDY POPULATION

This retrospective study was approved by the Institutional Review Board (IRB No. SC22RISI0113). We enrolled patients who complained of subjective memory impairment or cognitive impairment and underwent brain MRI at a single secondary referral center between June 2017 and August 2021. All the participants also underwent the Korean version of the Consortium to Establish a Registry for Alzheimer's Disease (CERAD-K) assessment for evaluation of cognitive function and were divided into the three groups; cognitively normal, mild cognitive impairment (MCI), and AD. One hundred thirty-nine patients met the criteria. However, one patient was excluded owing to inappropriate MRI with motion artifact. Finally, 138 patients (34 males and 104 females: mean age, 74.2 $\pm$ 7.0 years) were enrolled in our study. The definition of MCI was based on Peterson's criteria. Other supplementary information, such as total years of education, was collected by interviewing the patients and/or their caregivers.

MRI ACQUISITION

MRI was performed using a 3T unit (Magnetom Skyra; SIEMENS, Erlangen, Germany) with a body transmitting coil, and included T2-weighted imaging, fluid-attenuated inversion recovery (FLAIR) imaging, and a T2*-weighted gradient echo pulse sequence. All the included patients also underwent three-dimensional T1-weighted (3D T1WI) magnetization prepared rapid gradient echo (MPRAGE) imaging. A CMB was defined as a small punctate brain lesion showing loss of signal on the gradient echo pulse sequence. The imaging parameters for axi-

JOURNAL of THE KOREAN SOCIETY of RADIOLOGY

al FLAIR imaging were as follows: repetition time/echo time, 9000/76 ms; flip angle, 150°; matrix, 384 × 240; field of view (FOV), 199 × 220 mm; section thickness, 5 mm; scan time, 3 min 2 s. The imaging parameters for the axial gradient echo pulse sequence were as follows: repetition time/echo time, 752/19.9 ms; flip angle, 20°; matrix, 320 × 203; FOV, 199 × 220 mm; section thickness, 5 mm; scan time, 2 min 46 s. The imaging parameters for 3D T1WI MPRAGE were as follows: repetition time/echo time, 1860/2.53 ms; flip angle, 9°; TI, 984 ms; echo spacing, 7.2 ms; bandwidth, 220 Hz/pixel; averages, 1; matrix, 224 × 224; FOV, 224 × 224 mm; section thickness, 1 mm; time of acquisition 3 min 38 s.

IMAGING ANALYSES

Two radiologists (a faculty neuroradiologist and a radiology resident with 5 and 4 years of experience, respectively), blinded to the patients' clinical information, performed independent analyses of all the images for determining the location and number of CMBs in the lobar regions or deep white matter. The lobar regions included the frontal, parietal, temporal, and occipital lobes, while the deep white matter included the basal ganglia, thalamus, cerebellum, brain stem, and caudate nucleus. The number of CMBs greater than 30 were all recorded as 30. Two radiologists also assessed the degree of periventricular WMH (PVWMH) and deep WMH (DWMH) on the basis of the WMH visual rating system and ischemia classification system developed by the Clinical Research Center for Dementia of South Korea (20). The results of PVWMH and DWMH were later summed up to determine the WMH grade. PVWMH was classified into three grade as follows: P1 (cap or band < 5 mm), P2 (5 mm ≤ cap and band < 10 mm), and P3 (10 mm ≤ cap or band) (Fig. 1). DWMH were classified according to the size of deep white matter lesion as follows: D1 (maximal diameter < 10 mm), D2 (10 mm ≤ deep white matter lesion < 25 mm), and D3 (≥ 25 mm) (Fig. 2). WMH were classified by the combinations of PVWMH and DWMH as follows: minimal (D1P1 and D1P2), moderate (D2P1, D3P1, D2P2, and D1P3), and severe (D3P).

COGNITIVE LEVEL ASSESSMENT

All the included patients underwent assessments for cognitive function using the CERAD-K. The CERAD-K is a valid equivalent for the English version of the CERAD, clinical and neuropsychological assessment battery (21). This assessment includes eight tests, namely, Verbal Fluency, Modified Boston Naming, Mini-Mental State Examination (MMSE), Word List Memory, Constructional Praxis, Word List Recall, Word List Recognition, and Constructional Praxis Recall. These tests in the CERAD-K have been shown to successfully differentiate control individuals from dementia patients and AD patients with substantial interrater reliability (10). According to the CERAD-K, we categorized the groups as cognitive normal (CN), MCI, and AD.

STATISTICAL ANALYSES

Continuous variables (age, education level, and MMSE score) were assessed for variation among the cognitive groups using one-way analysis of variance (ANOVA) with post-hoc Bonferroni correction, and nominal variable (female sex) was analyzed for variation among the cognitive groups using the Kruskal–Wallis test with post-hoc Bonferroni correction. Normality was evaluated using the Shapiro–Wilk test. We also evaluated the correlation between the cog-

Fig. 1. MRI images show the representative cases of various degree of periventricular white matter hyperintensity according to the CREDOS white matter hyperintensity visual rating scale.
A. Mild degree of preventricular WMH (cap or band < 5 mm) on FLAIR image in a 71 year old female patient.
B. Moderate degree of preventricular WMH (5 mm ≤ cap and band < 10 mm) on FLAIR image in a 83 year old female patient.
C. Severe degree of preventricular WMH (10 mm ≤ cap or band) on FLAIR image in a 78 year old female patient.
D. Coronal T2 weighted image shows the cross-section at the yellow line of the periventricular WMH. Yellow line is located just above the roof of the lateral ventricles.
CREDOS = Clinical Research Center for Dementia of South Korea, FLAIR = fluid-attenuated inversion recovery, WMH = white matter hyperintensity

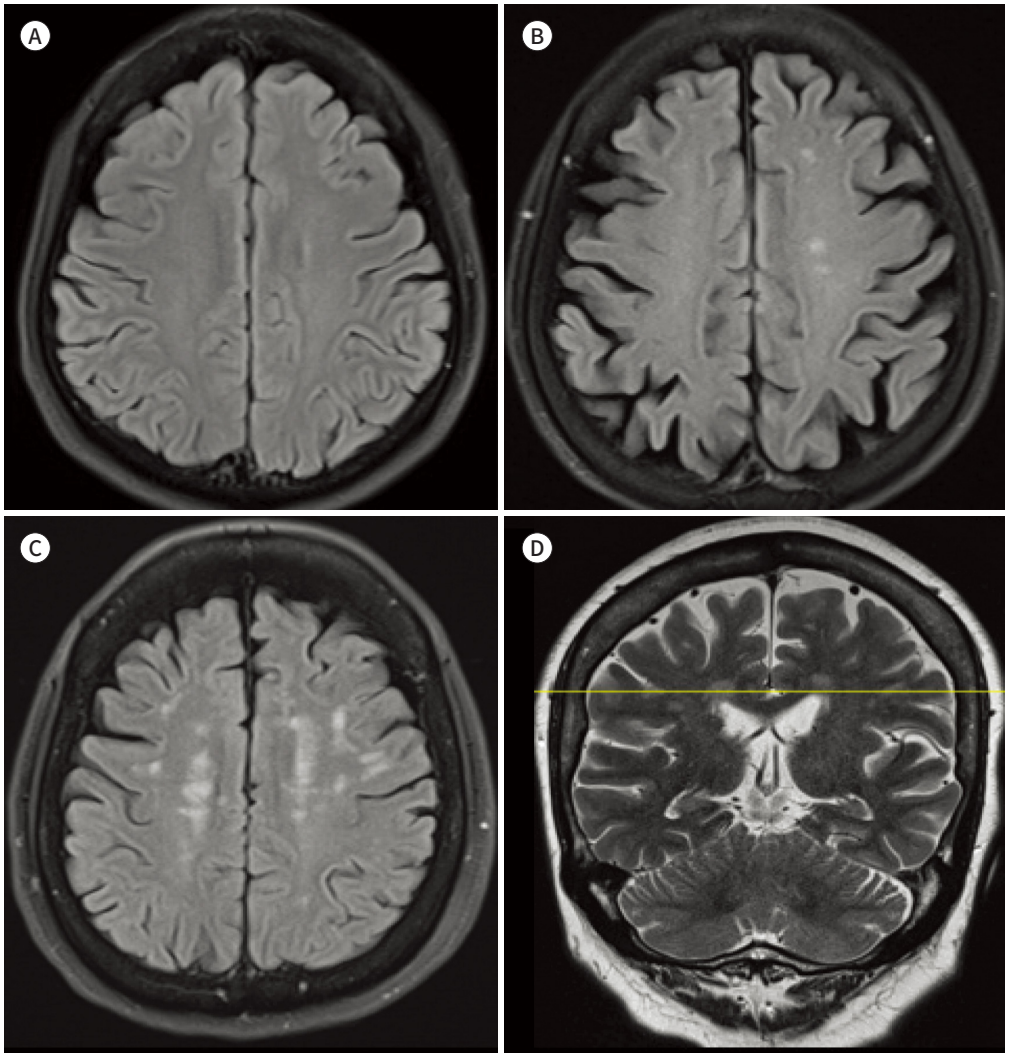

nitive function results (age, education level, and MMSE score) and imaging findings using *t*-test or Mann–Whitney test according to the normality results from the Shapiro–Wilk test (Supplementary Table 1 in the online-only Data Supplement). All the imaging findings were assessed using the Kruskal–Wallis test after Bonferroni correction among the three groups. A *p*-value < 0.0025 was considered statistically significant after Bonferroni correction.

The diagnostic performance of the imaging findings was assessed using receiver operating characteristic (ROC) curve analysis. The area under the ROC curve (AUC), sensitivity, specificity,

Fig. 2. MRI images show the representative cases of various degree of deep white matter hyperintensity according to the CREDOS white matter hyperintensity visual rating scale.
A. Mild degree of deep WMH (maximal deep white matter lesion diameter < 10 mm) on FLAIR image in a 62 year old female patient.
B. Moderate degree of deep WMH (10 mm ≤ maximal deep white matter lesion diameter < 25 mm) on FLAIR image in a 81 year old female patient.
C. Severe degree of deep WMH (maximal deep white matter lesion diameter ≥ 25 mm) on FLAIR image in a 75 year old female patient.
D. Coronal T2 weighted image shows the cross-section at the yellow line of the deep WMH. Yellow line is located two or more slices above the roof of the lateral ventricles.
CREDOS = Clinical Research Center for Dementia of South Korea, FLAIR = fluid-attenuated inversion recovery, WMH = white matter hyperintensity

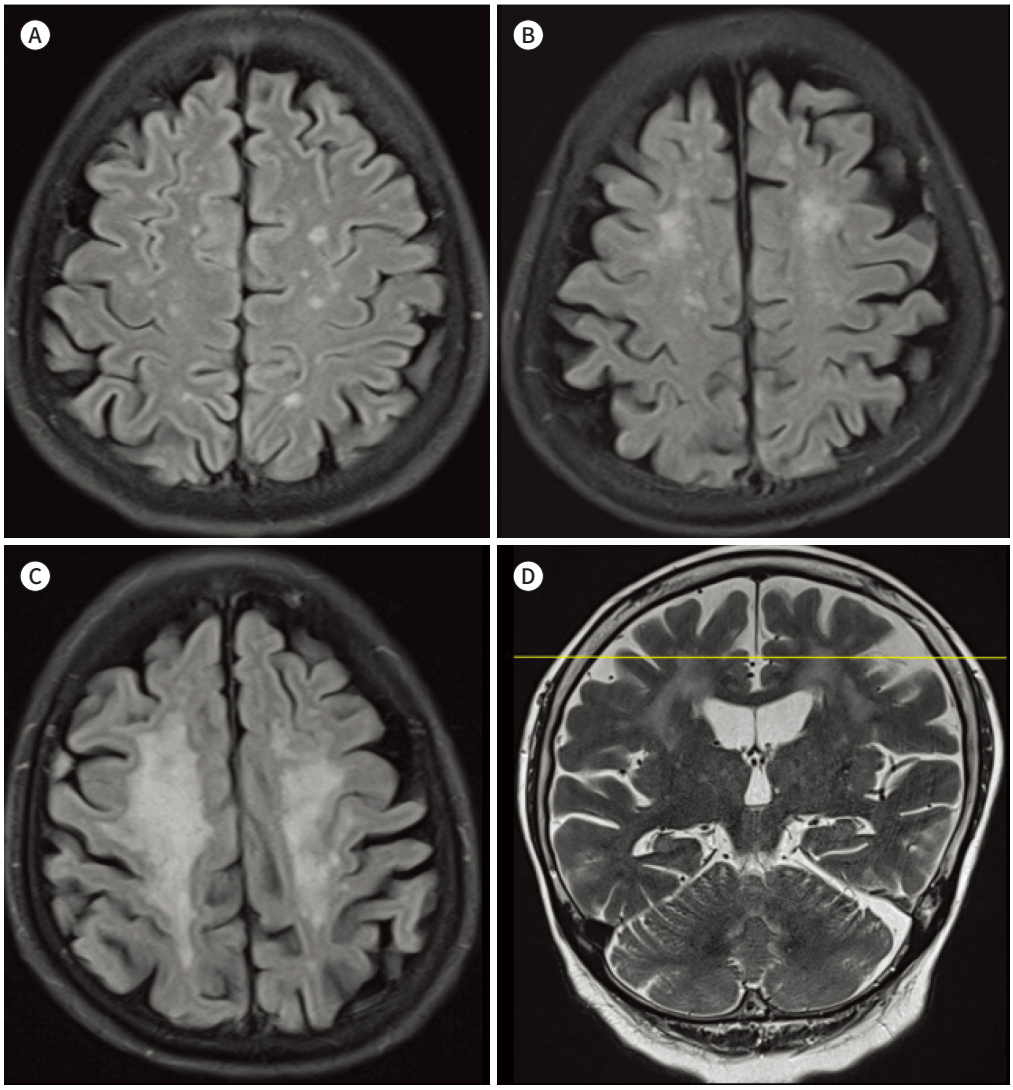

positive predictive value, negative predictive value, and accuracy were calculated. Inter-reader agreement was assessed using intraclass correlation coefficients. Comparison of the AUCs between the single imaging findings and combination was evaluated using DeLong's test. These analyses were performed using MedCalc (MedCalc version 20.014; Mariakerke, Belgium) and R statistical software (R version 4.0.2, R Foundation for Statistical Computing, Vienna, Austria).

RESULTS

Demographic findings of the included patients were demonstrated, and we evaluated the difference of the demographic findings for each group categorized to the cognitive level. (Table 1). Participants in the AD group were significantly older than those in the cognitively normal group (74.2 ± 7.0 vs. 74.1 ± 7.0 years, $p = 0.002$) and had lower MMSE scores than those in the cognitively normal and MCI groups, while the MCI group showed a lower MMSE score than the cognitively normal group ($p < 0.001$). The AD group showed a significantly higher positive rate in amyloid PET than the cognitively normal and MCI groups (all, $p < 0.001$). The three groups showed no significant differences in sex distribution and education level. The results of correlation between the cognitive function results (age, education level, and MMSE) and imaging findings are summarized in Supplementary Table 1 (in the online-only Data Supplement). Patients with CMBs demonstrated significantly older age than patients without CMBs (74.5 ± 11.0 vs. 73.1 ± 7.0, $p = 0.013$). Other cognitive function results demonstrated no difference according to the presence of CMBs or degree of WMH.

The intergroup difference in the imaging findings is summarized in Table 2. The AD group showed more frequent presence of CMBs with lobar and deep location than the cognitively normal and MCI groups ($p = 0.002$) (Figs. 3A, 4A). The AD group showed significantly higher scores for PVWMH, DWMH, and WMH than the cognitively normal group ($p = 0.005$, 0.001, and 0.001, respectively) (Figs. 3B, 4B), and the MCI group showed a significantly higher score for PVWMH than the cognitively normal group ($p < 0.001$). Imaging findings, including lobar CMBs and all WMH grades demonstrated moderate inter-reader agreements (0.40–0.56; Supplementary Table 2 in the online-only Data Supplement).

The results of the diagnostic performance of imaging findings for distinguishing between AD and non-AD (CN and MCI) groups are summarized in Table 3. The presence of lobar and deeply located CMBs showed significant diagnostic performance for differentiating between the AD and other groups (all, $p < 0.001$), with the lobar located CMBs showing the highest AUC value (AUC = 0.673 [95% confidence interval {CI}, 0.577–0.769], $p < 0.001$). The scores for PVWMH, DWMH, and WMH were significantly higher in the AD group ($p = 0.003$, 0.002, and 0.004), with the PVWMH score showing the highest AUC value (AUC = 0.649 [95% CI, 0.555–0.742], $p = 0.003$). The combination of lobar CMBs and the PVWMH score also showed signifi-

Table 1. Demographic Characteristics of the Study Population

	Total ($n = 138$)	CN ($n = 57$)	MCI ($n = 50$)	AD ($n = 31$)	p-Value	p-Value*	p-Value†	p-Value‡
Age (years)	74.2 ± 7.0	74.1 ± 7.0	74.2 ± 7.0	74.2 ± 7.1	0.014	0.149	0.002	0.119
Sex (female)	104 (75.4)	44 (77.2)	35 (70.0)	25 (80.7)	0.513	0.401	0.709	0.291
Education level (years)	10.9 ± 5.4	11.7 ± 4.6	10.9 ± 5.6	9.3 ± 6.0	0.127	0.398	0.037	0.231
MMSE	23.3 ± 5.7	23.4 ± 5.6	23.3 ± 5.6	22.8 ± 5.9	< 0.001	< 0.001	< 0.001	< 0.001

Data are presented as mean ± standard deviation or number (%). p-values are Bonferroni-corrected p-values. p refers to the statistical significance among the three groups.

*p refers to the statistical significance for the difference between the CN and MCI groups.

†p refers to the statistical significance for the difference between the CN and AD groups.

‡p refers to the statistical significance for difference between the MCI and AD groups.

AD = Alzheimer's disease, CN = cognitive normal, MCI = mild cognitive impairment, MMSE = Mini-Mental State Examination

Table 2. Association of MRI-Based Imaging Findings with Cognitive Decline

	Total (*n* = 138)	CN (*n* = 57)	MCI (*n* = 50)	AD (*n* = 31)	*p*-Value	*p*-Value*	*p*-Value†	*p*-Value‡
CMB	73 (52.9)	21 (36.8)	21 (42.0)	31 (100)	0.002	0.773	< 0.001	0.002
Lobar location	52 (37.7)	15 (26.3)	17 (34.0)	20 (64.5)	0.002	0.389	< 0.001	0.008
Deep location	21 (15.2)	6 (10.5)	4 (8.0)	11 (35.5)	0.002	0.656	0.005	0.002
PVWMH§	130 (94.2)	50 (87.7)	49 (98.0)	31 (100)	< 0.001	0.003	< 0.001	0.172
P1	92 (66.7)	43 (75.4)	33 (66.0)	16 (51.6)				
P2	23 (16.7)	4 (7.0)	9 (18.0)	10 (32.3)				
P3	15 (10.9)	3 (5.3)	7 (14.0)	5 (16.1)				
DWMH§	122 (88.4)	46 (80.7)	45 (90.0)	31 (25.4)	0.002	0.113	< 0.001	0.030
D1	110 (79.7)	44 (77.2)	41 (82.0)	25 (80.6)				
D2	8 (5.8)	1 (1.8)	3 (6.0)	4 (12.9)				
D3	4 (2.9)	1 (1.8)	1 (2.0)	2 (6.5)				
WMH§	119 (86.2)	43 (75.4)	45 (90.0)	31 (100)	< 0.001	0.014	< 0.001	0.137
Mild	101 (73.2)	40 (70.2)	37 (74.0)	24 (77.4)				
Moderate	14 (10.1)	2 (3.5)	7 (14.0)	5 (16.1)				
Severe	4 (2.9)	1 (1.8)	1 (2.0)	2 (6.5)				

Data are presented as number (%). *p*-values are Bonferroni-corrected *p*-values. *p* indicates statistically significant differences among the three groups.

**p* indicates the statistical significance for the difference between the CN and MCI groups.

†*p* indicates the statistical significance for the difference between the CN and AD groups.

‡*p* indicates the statistical significance for the difference between the MCI and AD groups.

§WMH scale is rated according to the CREDOS WMH visual rating scale.

AD = Alzheimer's disease, CMB = cerebral microbleed, CN = cognitive normal, CREDOS = Clinical Research Center for Dementia of South Korea, DWMH = deep white matter hyperintensity, MCI = mild cognitive impairment, PVWMH = periventricular white matter hyperintensity, WMH = white matter hyperintensity

Fig. 3. A 74-year-old male patient with subjective memory impairment, but with normal cognition on cognitive function test.

A. There is no definite microbleed on susceptibility-weighted imaging.

B. There is no significant white matter hyperintensity on FLAIR image.

FLAIR = fluid-attenuated inversion recovery

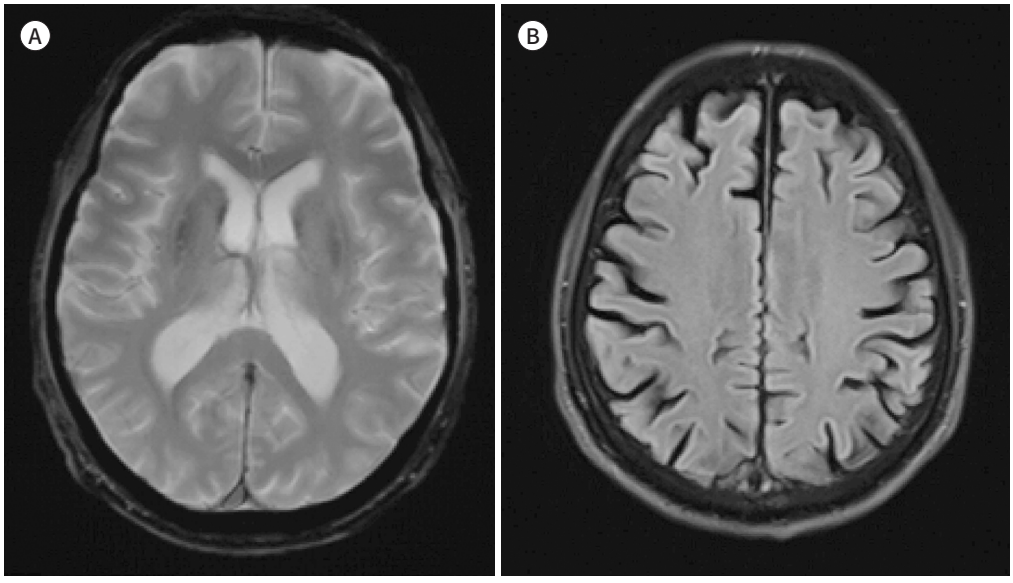

Fig. 4. An 83-year-old female patient with subjective memory impairment and Alzheimer's disease diagnosed on cognitive function test.
A. Susceptibility-weighted imaging shows multiple lobar microbleeds.
B. FLAIR image shows severe degree of white matter hyperintensity.
FLAIR = fluid-attenuated inversion recovery

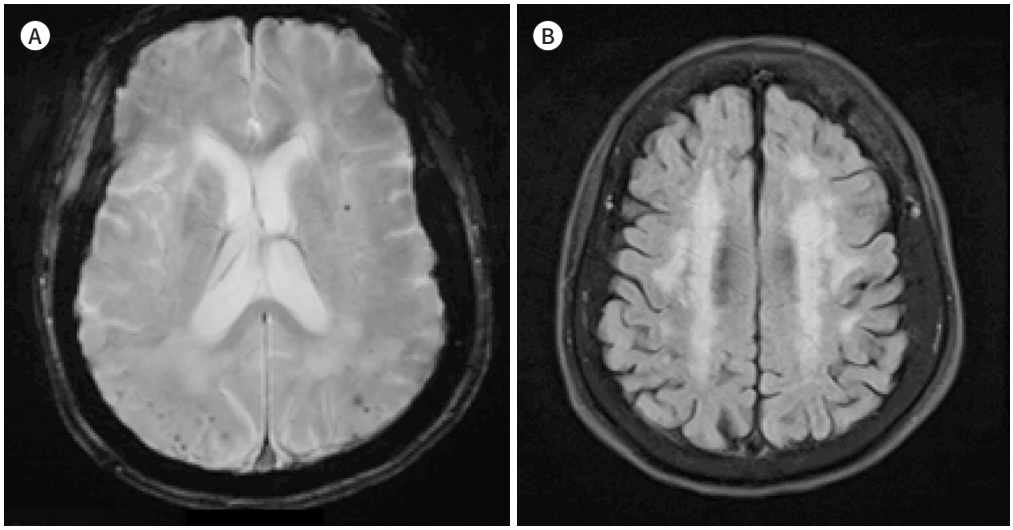

Table 3. Comparison of Diagnostic Performance in Differentiating Alzheimer's Disease from Non-Alzheimer's Disease Group

AD vs. Non-AD	AUC (95% CI)	*p*	Sensitivity (%)	Specificity (%)	PPV (%)	NPV (%)	Accuracy (%)
CMBs							
Lobar location	0.673 (0.578–0.769)	< 0.001	64.5	70.1	38.5	87.2	68.8
Deep location	0.631 (0.541–0.721)	< 0.001	35.5	90.7	52.4	82.9	78.3
WMH							
PVWMH scale	0.649 (0.555–0.742)	0.003	48.4	78.5	39.5	84.0	71.7
DWMH scale	0.629 (0.559–0.700)	0.002	100	15.0	100	43.1	34.1
Total scale	0.631 (0.556–0.707)	0.004	100	17.8	100	36.2	36.2
Combination							
Lobar location + PVWMH	0.702 (0.599–0.806)	< 0.001	64.5	71.0	39.2	87.4	69.6
CAA + PVWMH	0.665 (0.565–0.764)	0.001	32.3	95.3	66.7	82.9	81.2

Non-AD represents non-Alzheimer which is consisted of cognitively normal and mild cognitive impairment.
AD = Alzheimer's disease, AUC = area under the receiver operating characteristics curve, CAA = cerebral amyloid angiopathy, CI = confidence interval, CMB = cerebral microbleed, DWMH = deep white matter hyperintensity, NPV = negative predictive value, PPV = positive predictive value, PVWMH = periventricular white matter hyperintensity, WMH = white matter hyperintensity

cantly better diagnostic performance than the single finding alone (AUC = 0.702 [95% CI, 0.599–0.806], $p < 0.001$).

The results of the diagnostic performance for distinguishing between the CN and AD groups are shown in Table 4. The presence of lobar CMBs showed significant diagnostic performance for differentiating between the cognitively normal and AD groups ($p < 0.001$). Lobar located CMBs again showed the highest AUC value (AUC = 0.691 [95% CI, 0.588–0.794], $p < 0.001$). The PVWMH, DWMH, and WMH scores were significantly higher in the AD group (all, $p < 0.001$), with the PVWMH score showing the highest AUC value (AUC = 0.709 [95% CI, 0.615–0.804], $p < 0.001$). The combination of lobar CMBs and the PVWMH score showed sig-

Table 4. Comparison of Diagnostic Performance in Distinguishing Cognitively Normal Individuals from Patients with Alzheimer's Disease

AD vs. CN	AUC (95% CI)	*p*	Sensitivity (%)	Specificity (%)	PPV (%)	NPV (%)	Accuracy (%)
CMB							
Lobar location	0.691 (0.588–0.794)	< 0.001	64.5	73.7	57.1	79.2	70.5
Deep location	0.625 (0.530–0.719)	0.005	35.5	89.5	64.7	71.8	70.5
CAA	0.644 (0.557–0.731)	< 0.001	32.3	96.5	83.3	72.4	73.9
WMH							
PVWMH scale	0.709 (0.615–0.804)	< 0.001	48.4	87.7	68.2	75.8	73.9
DWMH scale	0.657 (0.581–0.732)	< 0.001	100	19.3	100	47.7	47.7
Total scale	0.681 (0.602–0.761)	< 0.001	100	24.5	100	51.1	51.1
Combination							
Lobar location + PVWMH	0.743 (0.639–0.846)	< 0.001	67.7	71.9	56.8	80.4	70.5
CAA + PVWMH	0.720 (0.625–0.815)	< 0.001	48.4	87.7	68.2	75.8	73.9

AD = Alzheimer's disease, AUC = area under the receiver operating characteristics curve, CAA = cerebral amyloid angiopathy, CI = confidence interval, CMB = cerebral microbleed, CN = cognitively normal, DWMH = deep white matter hyperintensity, NPV = negative predictive value, PPV = positive predictive value, PVWMH = periventricular white matter hyperintensity, WMH = white-matter hyperintensity

nificantly better diagnostic performance than the single finding alone (AUC = 0.743 [95% CI, 0.639–0.846], $p < 0.001$).

DISCUSSION

In this study, we observed that the presence of CMBs and higher WMH scores were associated with cognitive decline. Furthermore, the presence of CMBs, WMH scores, and certain combinations of these imaging findings showed better diagnostic performance for differentiating patients with cognitive decline. In particular, we found that the best diagnostic performance for distinguishing the AD group from the non-AD group was derived from the combination of lobar location of CMBs and a high score for WMH within the periventricular white matter.

Although previous studies have investigated the relationship between CMBs or WMH and cognitive decline, they focused on either CMBs or WMH alone in evaluating their associations with dementia (18). Previous studies have already demonstrated that CMBs, especially in large numbers, are related to decrease cognitive function in an otherwise healthy adult population (22-25). Furthermore, other studies demonstrated that the presence of microbleeds is associated with an increased risk for dementia (26). The findings of the present study are similar to the results of previous studies. On the other hand, the association of WMH with cognitive decline has been a topic of debate. Some studies suggested that WMH is also associated with an increased risk of developing AD (27), while others observed no apparent relationship (28). In our study, we demonstrated that higher PVWMH, DWMH, and WMH scores showed a significant correlation with the rate of cognitive decline. Although CMBs or WMH alone have been frequently studied for their associations with cognitive function, combinations of these two findings are not as widely investigated. Thus, the most notable finding in our study is that a combination of subtypes of CMBs and WMH (lobar located CMB + PVWMH) showed better diagnostic performance for differentiating AD in comparison with CMBs or WMH alone.

Recent studies evaluated the diagnostic performance of cognitive decline using advanced

imaging techniques, including volumetric analysis, functional MRI, and PET (8-11). These methods showed promising results and can be used as diagnostic tools for detecting AD. Relatively, conventional imaging findings showed inferior performance for evaluating patients with cognitive decline. Although conventional imaging findings showed a relatively lower clinical impact for detecting cognitive decline, they may have additive values for estimating visualized change during follow-up and provide the rationale for tertiary hospital referral. In real-world clinical practice, most primary or secondary hospitals may have limitations to evaluate patients with cognitive decline because of low accessibility or utilization of advanced imaging techniques or volumetric analysis even though advanced imaging techniques and artificial interest-based volumetric analysis are widely used for detecting a cognitive decline in tertiary or referral centers. Therefore, simple imaging findings by visual assessment can help physicians in primary or secondary hospitals for estimating the probability of cognitive decline and selecting patients for referral to tertiary hospitals for performing advanced imaging techniques.

The presence of CMBs and high grade of WMH can be considered simple imaging findings for estimating patients with cognitive decline. Since small-vessel disease is known to be the primary cause of blood brain barrier (BBB) disruption (29), this vicious cycle accelerates AD progression. Multiple studies have reported significant associations between small-vessel disease and AD based on these possible pathways. CMBs and WMH demonstrated association with small-vessel disease in AD, which can be explained on the basis of cerebrovascular concepts (30-33). The association between small-vessel disease and CMBs is explained by the perivascular edema and the release of toxic materials into the brain parenchyma (13-15, 34-37). Several studies have also explained the cause of WMH on the basis of small-vessel disruption (30, 32, 38). Small-vessel disease, which involves BBB breakage, small infarctions, and demyelination, causes cerebral blood flow reduction. Since white matter is a watershed area and vulnerable to hypoxia and hypoperfusion, these reductions in cerebral blood flow cause WMH (39, 40). These imaging findings indicating the physiologic causes or outcomes of cerebrovascular disease may facilitate evaluations of cognitive decline. Therefore, conventional imaging findings (CMBs and WHM) had an additive value for estimating cognitive decline according to the concept of small-vessel disease.

This study had several limitations. First, the study was a retrospective study from a single secondary referral center in a community with a rather high socioeconomic status, and our study included a small and heterogeneous sample. Therefore, these factors might introduce inevitable selection bias. Second, we assessed only gradient echo pulse sequences to identify the presence and numbers of CMBs. Since gradient echo pulse sequences have poorer spatial resolution than susceptibility-weighted imaging (SWI), they may show limited precision for assessment of CMBs. In future studies, SWI assessment should be considered for better depiction of the true brain status in microbleeds. Third, the retrospective nature of the study was associated with some inherent limitations. Fourth, although several important factors can alter patients' cognitive levels, including physical activity, alcohol consumption habits, and previous medical history (12, 38), none of these factors could be effectively controlled in this study population. Finally, similar to patients with CMBs who were significantly older than patients without CMBs, the AD group had significantly older patients than the CN group. There-

fore, age could be considered a covariate variable for evaluating diagnostic performance in differentiating the AD group from the CN group. Further studies following age matching should be performed to evaluate the accurate diagnostic performance for detecting AD.

In conclusion, we found that the presence of CMBs and WMH was a useful predictor for estimating cognitive decline and rationale for patient referral to tertiary hospitals. In particular, combined imaging findings (lobar CMB + PVWMH) showed good diagnostic performance in distinguishing AD from non-AD groups. Therefore, we highlight that these imaging findings on conventional brain MRI can provide additional values for evaluating patients with cognitive decline, especially in primary care centers.

Supplementary Materials

The online-only Data Supplement is available with this article at http://doi.org/10.3348/jksr.2023.0065.

Author Contributions

Conceptualization, L.M.K.; data curation, B.J.Y., L.M.K.; formal analysis, B.J.Y., L.M.K.; investigation, L.M.K.; methodology, B.J.Y., L.M.K.; project administration, L.M.K.; resources, L.M.K.; supervision, L.M.K., J.S.L.; validation, L.M.K., J.S.L.; writing—original draft, B.J.Y., L.M.K.; and writing—review & editing, B.J.Y., L.M.K.

Conflicts of Interest

The authors have no potential conflicts of interest to disclose.

Funding

None

REFERENCES

1. Blazer DG, Yaffe K, Karlawish J. Cognitive aging: a report from the institute of medicine. *JAMA* 2015;313:2121-2122
2. Mintun MA, Lo AC, Duggan Evans C, Wessels AM, Ardayfio PA, Andersen SW, et al. Donanemab in early Alzheimer's disease. *N Engl J Med* 2021;384:1691-1704
3. Busche MA, Hyman BT. Synergy between amyloid-β and tau in Alzheimer's disease. *Nat Neurosci* 2020;23:1183-1193
4. Demattos RB, Lu J, Tang Y, Racke MM, Delong CA, Tzaferis JA, et al. A plaque-specific antibody clears existing β-amyloid plaques in Alzheimer's disease mice. *Neuron* 2012;76:908-920
5. Selkoe DJ, Hardy J. The amyloid hypothesis of Alzheimer's disease at 25 years. *EMBO Mol Med* 2016;8:595-608
6. Petersen RC, Lopez O, Armstrong MJ, Getchius TSD, Ganguli M, Gloss D, et al. Practice guideline update summary: mild cognitive impairment: report of the guideline development, dissemination, and implementation subcommittee of the American Academy of Neurology. *Neurology* 2018;90:126-135
7. Folstein MF, Folstein SE, McHugh PR. "Mini-mental state". A practical method for grading the cognitive state of patients for the clinician. *J Psychiatr Res* 1975;12:189-198
8. Steinbart D, Yaakub SN, Steinbrenner M, Guldin LS, Holtkamp M, Keller SS, et al. Automatic and manual segmentation of the piriform cortex: method development and validation in patients with temporal lobe epilepsy and Alzheimer's disease. *Hum Brain Mapp* 2023;44:3196-3209
9. Chandra A, Dervenoulas G, Politis M; Alzheimer's Disease Neuroimaging Initiative. Magnetic resonance imaging in Alzheimer's disease and mild cognitive impairment. *J Neurol* 2019;266:1293-1302
10. Mueller SG, Schuff N, Weiner MW. Evaluation of treatment effects in Alzheimer's and other neurodegenerative diseases by MRI and MRS. *NMR Biomed* 2006;19:655-668
11. Rowley PA, Samsonov AA, Betthauser TJ, Pirasteh A, Johnson SC, Eisenmenger LB. Amyloid and tau PET imaging of Alzheimer disease and other neurodegenerative conditions. *Semin Ultrasound CT MR* 2020;41:

572-583
12. Cannistraro RJ, Badi M, Eidelman BH, Dickson DW, Middlebrooks EH, Meschia JF. CNS small vessel disease: a clinical review. *Neurology* 2019;92:1146-1156
13. Li Q, Yang Y, Reis C, Tao T, Li W, Li X, et al. Cerebral small vessel disease. *Cell Transplant* 2018;27:1711-1722
14. Wardlaw JM, Smith C, Dichgans M. Mechanisms of sporadic cerebral small vessel disease: insights from neuroimaging. *Lancet Neurol* 2013;12:483-497
15. Shi Y, Wardlaw JM. Update on cerebral small vessel disease: a dynamic whole-brain disease. *Stroke Vasc Neurol* 2016;1:83-92
16. Patel B, Markus HS. Magnetic resonance imaging in cerebral small vessel disease and its use as a surrogate disease marker. *Int J Stroke* 2011;6:47-59
17. Norrving B. Evolving concept of small vessel disease through advanced brain imaging. *J Stroke* 2015;17:94-100
18. Graff-Radford J, Arenaza-Urquijo EM, Knopman DS, Schwarz CG, Brown RD, Rabinstein AA, et al. White matter hyperintensities: relationship to amyloid and tau burden. *Brain* 2019;142:2483-2491
19. Cordonnier C, van der Flier WM, Sluimer JD, Leys D, Barkhof F, Scheltens P. Prevalence and severity of microbleeds in a memory clinic setting. *Neurology* 2006;66:1356-1360
20. Noh Y, Lee Y, Seo SW, Jeong JH, Choi SH, Back JH, et al. A new classification system for ischemia using a combination of deep and periventricular white matter hyperintensities. *J Stroke Cerebrovasc Dis* 2014;23:636-642
21. Lee JH, Lee KU, Lee DY, Kim KW, Jhoo JH, Kim JH, et al. Development of the Korean version of the consortium to establish a registry for Alzheimer's disease assessment packet (CERAD-K): clinical and neuropsychological assessment batteries. *J Gerontol B Psychol Sci Soc Sci* 2002;57:P47-P53
22. Poels MM, Ikram MA, van der Lugt A, Hofman A, Niessen WJ, Krestin GP, et al. Cerebral microbleeds are associated with worse cognitive function: the Rotterdam scan study. *Neurology* 2012;78:326-333
23. Qiu C, Cotch MF, Sigurdsson S, Jonsson PV, Jonsdottir MK, Sveinbjrnsdottir S, et al. Cerebral microbleeds, retinopathy, and dementia: the AGES-Reykjavik study. *Neurology* 2010;75:2221-2228
24. Takashima Y, Mori T, Hashimoto M, Kinukawa N, Uchino A, Yuzuriha T, et al. Clinical correlating factors and cognitive function in community-dwelling healthy subjects with cerebral microbleeds. *J Stroke Cerebrovasc Dis* 2011;20:105-110
25. Yakushiji Y, Noguchi T, Hara M, Nishihara M, Eriguchi M, Nanri Y, et al. Distributional impact of brain microbleeds on global cognitive function in adults without neurological disorder. *Stroke* 2012;43:1800-1805
26. Akoudad S, Wolters FJ, Viswanathan A, de Bruijn RF, van der Lugt A, Hofman A, et al. Association of cerebral microbleeds with cognitive decline and dementia. *JAMA Neurol* 2016;73:934-943
27. Debette S, Markus HS. The clinical importance of white matter hyperintensities on brain magnetic resonance imaging: systematic review and meta-analysis. *BMJ* 2010;341:c3666
28. Lee JH, Olichney JM, Hansen LA, Hofstetter CR, Thal LJ. Small concomitant vascular lesions do not influence rates of cognitive decline in patients with Alzheimer disease. *Arch Neurol* 2000;57:1474-1479
29. Wardlaw JM. Blood-brain barrier and cerebral small vessel disease. *J Neurol Sci* 2010;299:66-71
30. Duering M, Csanadi E, Gesierich B, Jouvent E, Hervé D, Seiler S, et al. Incident lacunes preferentially localize to the edge of white matter hyperintensities: insights into the pathophysiology of cerebral small vessel disease. *Brain* 2013;136:2717-2726
31. Hommet C, Mondon K, Constans T, Beaufils E, Desmidt T, Camus V, et al. Review of cerebral microangiopathy and Alzheimer's disease: relation between white matter hyperintensities and microbleeds. *Dement Geriatr Cogn Disord* 2012;32:367-378
32. Shi Y, Thrippleton MJ, Makin SD, Marshall I, Geerlings MI, de Craen AJM, et al. Cerebral blood flow in small vessel disease: a systematic review and meta-analysis. *J Cereb Blood Flow Metab* 2016;36:1653-1667
33. Zhang CE, Wong SM, Uiterwijk R, Backes WH, Jansen JFA, Jeukens CRLPN, et al. Blood-brain barrier leakage in relation to white matter hyperintensity volume and cognition in small vessel disease and normal aging. *Brain Imaging Behav* 2019;13:389-395
34. Holland CM, Smith EE, Csapo I, Gurol ME, Brylka DA, Killiany RJ, et al. Spatial distribution of white-matter hyperintensities in Alzheimer disease, cerebral amyloid angiopathy, and healthy aging. *Stroke* 2008;39:1127-1133
35. Hartz AM, Bauer B, Soldner EL, Wolf A, Boy S, Backhaus R, et al. Amyloid-β contributes to blood-brain barrier

leakage in transgenic human amyloid precursor protein mice and in humans with cerebral amyloid angiopathy. *Stroke* 2012;43:514-523
36. Wardlaw JM, Smith EE, Biessels GJ, Cordonnier C, Fazekas F, Frayne R, et al. Neuroimaging standards for research into small vessel disease and its contribution to ageing and neurodegeneration. *Lancet Neurol* 2013;12:822-838
37. Rizvi B, Narkhede A, Last BS, Budge M, Tosto G, Manly JJ, et al. The effect of white matter hyperintensities on cognition is mediated by cortical atrophy. *Neurobiol Aging* 2018;64:25-32
38. Pantoni L. Cerebral small vessel disease: from pathogenesis and clinical characteristics to therapeutic challenges. *Lancet Neurol* 2010;9:689-701
39. De Silva TM, Miller AA. Cerebral small vessel disease: targeting oxidative stress as a novel therapeutic strategy? *Front Pharmacol* 2016;7:61
40. Wu YT, Prina AM, Brayne C. The association between community environment and cognitive function: a systematic review. *Soc Psychiatry Psychiatr Epidemiol* 2015;50:351-362

인지기능 저하평가를 위한 MR 영상 소견 조합의 진단능

변진영 · 이민경* · 정소령

목적 인지기능 저하를 진단하기 위해서 자기공명영상을 이용한 영상 소견의 진단능을 평가하였다.

대상과 방법 총 138명의 주관적인 인기지능 저하를 호소하며, MRI 검사를 시행한 환자를 대상으로 하였다. 이 환자 그룹은 신경정신학적 평가를 통해 알츠하이머군과 비알츠하이머군으로 분류되었다. 우리는 이들의 white matter hyperintensity와 cerebral microbleed를 평가하였으며, Kruskal- Wallis test를 통해 그룹 간의 비교를, receiver operating characteristic (이하 ROC)를 통해 영상학적 소견의 진단능을 평가하였다.

결과 인지기능 정상인 경우와 경도인지장애 환자와 비교해서 알츠하이머 환자에서 엽 혹은 심부 미세출혈이 빈번하게 관찰되었으며, 심한 심부 혹은 뇌실주위, 전체 백질 신호강도 또한 인지기능 정상에 비해서 알츠하이머 환자에서 많이 관찰되었다. 알츠하이머 환자와 다른 환자 그룹(정상 혹은 경도인지장애)을 비교할 때 엽미세출혈과 뇌실주위 뇌백질 신호강도 증가가 같이 존재하는 경우 가장 높은 진단능을 보였다(area under the ROC curve = 0.702 [95% 신뢰구간: 0.599–0.806], $p < 0.001$).

결론 자기공명영상에서 확인한 영상 소견을 바탕으로 인지기능 저하의 진단능을 평가하였다. 인지기능 저하의 진단에 있어서 엽미세출혈과 뇌실주위 뇌백질 신호강도 증가가 같이 존재하는 경우에 높은 진단능을 보였으며, 이러한 소견을 바탕으로 인지기능 저하를 진단하는 데 있어 영상 소견이 도움을 줄 수 있을 것이라는 가능성을 보여주었다.

가톨릭대학교 의과대학 여의도성모병원 영상의학과